

Witnessing Disorder in Quantum Magnets

Snigdha Sabharwal,^{1,*} Tokuro Shimokawa,¹ and Nic Shannon¹

¹*Theory of Quantum Matter Unit, Okinawa Institute of Science and Technology Graduate University, Onna-son, Okinawa 904-0412, Japan*

(Dated: August 1, 2024)

There are no clean samples in nature. Therefore, when we come to discuss the entanglement properties of quantum materials, the effects of disorder must be taken into account. This question is of particular interest for high-entangled states, such as quantum spin liquids, which lie outside the Landau paradigm for classifying phases of matter. In this work, we explore what experimentally-accessible measures, in the form of concurrence, residual tangle and quantum Fisher information, can teach us about the entanglement in the presence of disorder. As a representative example, we consider the Tomonaga-Luttinger liquids (TLL) and disorder-driven random singlet (RS) states found in antiferromagnetic quantum spin chains. Using quantum Fisher information and residual tangle, we demonstrate that both TLL and RS states exhibit multi-partite entanglement. In the case of the RS state, we attribute this to entanglement localized below a crossover length scale. We further show that the order of disorder average matters in calculating measures like concurrence, and that this can lead to false inferences when interpreting experiment. None the less, correctly interpreted, these witnesses provide useful information about the effects of disorder. We explore how information about the central charge of the TLL can be extracted from the low-temperature behavior of concurrence, and conjecture that this analysis can be extended to the effective central charge of the RS state. Finally, we establish how RS and TLL states can be distinguished through the growth of multi-partite entanglement, as witnessed by the equal-time structure factor. These results establish that, used carefully, experiments based on entanglement witnesses can provide important information about quantum spin systems in the presence of disorder.

I. INTRODUCTION

How does disorder affect entanglement within quantum materials? Can we quantify such effects experimentally? In nature, all materials possess a certain degree of disorder. Thus, when trying to understand any phase of matter, the role of disorder is an important factor to take into consideration. Disorder or randomness is especially problematic when trying to identify quantum spin liquid (QSL) states within candidate materials. This question arises in the context of many different materials, including κ -ET₂Cu₂(CN)₃ [1–8], ZnCu₃(OD)₆Cl₂ (Herbertsmithite) [7, 9–18], YbMgGaO₄ [19–22], H₃LiIr₂O₆ [23–25], etc. Here the challenge lies in being able to distinguish quantum fluctuations from disorder-induced ones. This puts into question whether it is the QSL or some disorder induced state realized within these materials?

Entanglement is a valuable resource to identify states such as QSLs [26]. Intuitively, one expects disorder, which localizes correlations, to have an effect on entanglement. The key issue, however, is whether this information can be accessed experimentally. Unlike cold atom systems where non local measures like (Rényi) entanglement entropy are accessible [27, 28], the same does not extend to condensed matter systems. Consequently, only limited information about the underlying state can typically be accessed experimentally. It is thus

important to determine if useful information about the entanglement structure can be obtained within experimental constraints. Can we do so by making use of experimentally-accessible entanglement measure [29–59], for instance?

In this study, we explore how measures based on entanglement witnesses can be used to distinguish the different phases which arise in quantum spin systems with and without disorder. As a representative example, we consider the $S = 1/2$ Heisenberg (XXX) spin chain with and without bond disorder. The competing phases in this case are the Tomonaga Luttinger liquid (TLL) [60] found in the absence of disorder, and the random singlet (RS) state realised for arbitrarily weak bond disorder [61–65]. We consider three different measures, namely concurrence [66, 67], tangle [68] and quantum Fisher information (QFI) [40, 48], all of which have previously been discussed in the context of experiment [53, 55, 57, 59], and use exact diagonalization to explore how each of these behaves in the TLL and RS states.

From this analysis, we conclude:

- Both the TLL and RS state are multi-partite entangled. In the TLL, multi-partite entanglement is present at all length scales. However, in the RS state, multi-partite entanglement is restricted to clusters smaller than a crossover lengthscale, beyond which the effects of disorder become relevant.
- Convex roof functions, like concurrence, are sensitive to the order in which disorder-averages are

* snigdha.sabharwal@oist.jp

calculated. In practice, this means that the distribution of concurrence in real space cannot be used to distinguish TLL from RS in experiments on systems with quenched disorder.

- Information about the central charge of the TLL can be extracted from the low-temperature behaviour of concurrence. We conjecture that this analysis can be extended to the effective central charge of the RS state, and show how this approach could be used to distinguish TLL from RS in the presence of quenched disorder.
- The temperature-dependence of multi-partite entanglement, as witnessed by quantum Fisher information (QFI), provides a robust means of probing the effect of disorder on quantum spin systems. In the case of quantum spin chains, this provides a clear distinction between the TLL and RS states which can be accessed in experiment.

For our investigations, we employed exact diagonalization (ED) and the thermal pure quantum (TPQ) methods [69–72]. Moreover, throughout this Article we work in the units where $\hbar = 1$ and $k_B = 1$.

The remainder of the Article is structured as follows. In Sec. II, we start out by giving a brief background on how one can access and/or detect entanglement in a limited setting using only one and two point spin-correlation functions. In our work, we employ concurrence to characterize the pairwise entanglement, residual tangle (RT) to detect the presence of multi-partite entanglement and the QFI to characterize the depth of multi-partite entanglement within the state. The subtleties, where they arise, are explained along the way.

In Sec. III, we detail our notation for evaluating averages. Sec. IV reviews key results related to the two states under investigation: the TLL and RS states. Sec. V introduces the model, disorder, and parameters used to investigate the entanglement structure of these states. Following which, in Sec. VI we present our zero temperature results for concurrence, RT and QFI. Sec. VII explores the finite temperature behavior of concurrence and equal time structure factor as witnesses. Here we address the subtleties involved with disorder averaging when dealing with convex roof measures like concurrence. We also discuss how to access the central charge for these states using concurrence and demonstrate the utility of using a multi-partite entanglement witness like equal-time structure factor as a probe for observing disorder effects.

In Sec. VIII, we discuss at length the nature of entanglement in the RS state, explaining the observed multi-partite entanglement and its origins. Finally, we conclude our findings in Sec. IX.

II. ACCESSING ENTANGLEMENT IN MANY BODY QUANTUM SYSTEMS

Entanglement in the modern perspective is thought of as a resource, one that can be used for quantum computation and information processing [73]. To this end, an important goal within quantum information is to quantify how entangled a state is? Unfortunately doing so is quite challenging and aside from a few special cases there is no solution as of yet. Even figuring out given a density matrix whether a state is separable or entangled, computationally, turns out to be very complex: in fact it is an *NP-hard* problem [74].

On the other hand, when it comes to quantifying or detecting entanglement in experimental settings, especially in condensed matter, the challenge diverges from computational complexity to practical feasibility. With a large number of particles involved, a complete state reconstruction by techniques like quantum state tomography is not possible. Thus quantifying entanglement using entanglement entropy Eq. (1),

$$E(|\phi_{AB}\rangle) = S(\rho_A) = -\text{Tr} \rho_A \log(\rho_A), \quad (1)$$

where ρ_A corresponds to a reduced density matrix obtained by tracing out subsystem B

$$\rho_A = \text{Tr}_B(|\phi_{AB}\rangle\langle\phi_{AB}|), \quad (2)$$

is not an option.

So how does one quantify or detect entanglement in a way that is experimentally tractable for condensed matter systems? One strategy is to employ *entanglement witnesses* [35, 36], which are observables that provide a means to detect entanglement in situations where one possesses limited information about the state. These observables violate certain bounds to indicate the existence of a bi-partite or multi-partite entanglement.

In what we follows, we briefly review the concepts and definitions needed to understand this Article. We start by introducing the concept of entanglement, and then then introduce three entanglement witness-based measures: concurrence [66, 67], tangle [68], and quantum Fisher information (QFI) [40, 48]. The advantage of using these measures is that they can be measured from spin correlations and structure factors which are readily accessible by techniques like INS.

A. Entanglement essentials

A bi-partite mixed state ρ is said to separable if it can be expressed as

$$\rho = \sum_i p_i \rho_i^A \otimes \rho_i^B, \quad (3)$$

and entangled otherwise. When A and B comprise of a single element, we use the term 2-partite for clarity. For

example, A and B could correspond to $S = 1/2$ particles on a lattice site. The product state

$$\rho = \rho^A \otimes \rho^B, \quad (4)$$

is a special case of the separable state.

The classification of multi-partite states is slightly more subtle since there are many inequivalent ways to partition the system [40, 75]. Let us begin by imagining a pure state comprised of N particles which we partition into M blocks. Now, if all the blocks are of size at most k , then the state is termed k -*producible* i.e.,

$$|\psi_{k\text{-prod}}\rangle = \otimes_{l=1}^M |\psi_l\rangle \text{ such that } N_l \leq k \forall l, \quad (5)$$

where it is understood

$$\sum_l N_l = N, \quad (6)$$

A state is k -*partite entangled* if it is k -producible but not $(k-1)$ -producible which translates to

$$|\psi_{k\text{-ent}}\rangle = \otimes_{l=1}^M |\psi_l\rangle \text{ such that } N_l = k \text{ for some } l, \quad (7)$$

i.e., there exists a non-factorizable state $|\psi_l\rangle$ with exactly $N_l = k$ particles. A mixed state $\rho_{k\text{-prod}}$ is said to be k -producible if it can be written as a convex mixture of k -producible pure states,

$$\rho_{k\text{-prod}} = \sum_r p_r |\psi_{k\text{-prod}}^r\rangle \langle \psi_{k\text{-prod}}^r| \quad (k_l \leq k \forall k), \quad (8)$$

where

$$p_r > 0 \text{ and } \sum_r p_r = 1. \quad (9)$$

Having introduced the necessary terminology, we are in a good position to introduce the entanglement measures. We focus our investigation towards those suited for $S = 1/2$ particles. There do exist generalizations of the measures discussed for arbitrary spin quanta but we do not discuss them here. An exception is the QFI that we discuss in Sec. IID

B. Concurrence

Concurrence quantifies the pairwise entanglement between two $S = 1/2$ particles. This could be in a system of only two or many $S = 1/2$ particles. For a mixed state ρ_{ij} shared between them where i and j are the indices pointing to the particles in question, it was shown [66, 67] to have the following relationship

$$C_{ij} \equiv C(\rho_{ij}) = \max\{0, \lambda_1 - \lambda_2 - \lambda_3 - \lambda_4\}, \quad (10)$$

Here, λ 's correspond to the square root of the eigenvalues of a non-Hermitian matrix

$$\rho_{ij} \tilde{\rho}_{ij} |v_\lambda\rangle = \lambda^2 |v_\lambda\rangle, \quad (11)$$

arranged in descending order, with

$$\tilde{\rho}_{ij} = (\sigma_y \otimes \sigma_y) \rho_{ij}^* (\sigma_y \otimes \sigma_y), \quad (12)$$

being a spin-flipped state and $*$ denoting the complex conjugation operation performed in the computational basis.

Following this definition, concurrence ranges from 0 corresponding to a separable state to 1, a maximally entangled Bell state. It quantifies the degree of 2-partite entanglement regardless of whether the state is pure or mixed. Thus, it remains a good measure of entanglement even at finite temperature. The practical advantage of using concurrence is that it is related to spin correlations [76, 77] and thus a very useful tool to access the 2-partite entanglement in the system. For instance, a $SU(2)$ symmetric system, a $S = 1/2$ spin chain Eq. (38) for example, is given by [77]

$$C_{ij} = 2 \max \left\{ 0, 2|g_{ij}^{zz}| - \left| \frac{1}{4} + g_{ij}^{zz} \right| \right\}, \quad (13)$$

where

$$g_{ij}^{zz} = \langle S_i^z S_j^z \rangle. \quad (14)$$

In a system with more than two particles one should note that vanishing concurrence doesn't imply absence of higher partite entanglement. Often, one also uses the *two-tangle* [68, 78, 79]

$$\tau_{2,i} = \sum_{j \neq i} C_{ij}^2, \quad (15)$$

as a measure of pairwise entanglement which characterizes all possible pairwise entanglement within a many partite system.

C. Residual Tangle

Residual tangle (RT) [68, 79] is a measure that accesses entanglement beyond the pairwise setting, in other words, a multi-partite measure. It is defined as the difference between one-tangle and the sum of pairwise entanglement measured via the two-tangle,

$$\tau_{3,i} = \tau_{1,i} - \tau_{2,i}, \quad (16)$$

where

$$\tau_{1,i} = 1 - 4 \sum_{\alpha=\{x,y,z\}} \langle S_i^\alpha \rangle^2, \quad (17)$$

is the one-tangle characterizing the entanglement of a $S = 1/2$ particle indexed by i with the rest of the system.

Strictly, $\tau_{1,i}$ serves as a measure of entanglement only for pure states. By extension, the same is true of $\tau_{3,i}$. And as a consequence, the interpretation of RT as an entanglement measure becomes inapplicable at finite temperatures. Moreover, although a nonzero RT suggests the presence of multi-partite entanglement, a zero RT does not necessarily indicate its absence.

D. Quantum Fisher Information

The measures discussed previously are very useful, however they come with the limitations of being unable to access multi-partite entanglement, or become invalid as measures at finite temperatures. A measure that does take care of both these issues is the quantum Fisher information (QFI). For a mixed state described using the spectral decomposition

$$\rho = \sum_k p_k |k\rangle\langle k|, \quad (18)$$

such that $p_k > 0$ and $\sum_k p_k = 1$, the QFI is specified, with respect to some operator \hat{O} , as

$$F_Q[\rho, \hat{O}] = 2 \sum_{k,k'} \frac{(p_k - p_{k'})^2}{p_k + p_{k'}} |\langle k|\hat{O}|k'\rangle|^2, \quad (19)$$

which for pure states simplifies to

$$F_Q[|\psi\rangle, \hat{O}] = 4(\Delta\hat{O})^2 = 4\left(\langle\hat{O}^2\rangle - \langle\hat{O}\rangle^2\right). \quad (20)$$

Thus, for pure states, it simplifies to the variance of \hat{O} upto proportionality. At finite temperature, for a system in thermodynamic equilibrium, the probability p_k Eq. (18) corresponds to the occupation probability as ascribed by the canonical ensemble

$$p_k = \exp(-E_k\beta)/Z, \quad (21)$$

where Z corresponds to the partition function and β is the inverse temperature. For this case, the QFI density

$$f_Q = F_Q/N, \quad (22)$$

can be accessed

$$f_Q(\beta) = \frac{4}{\pi} \int_0^\infty d\omega \tanh\left(\frac{\omega\beta}{2}\right) \chi''(\beta, \omega), \quad (23)$$

from the dissipative part of dynamic susceptibility [48], $\chi''(\beta, \omega)$ defined as,

$$\chi(\beta, \omega) = \frac{i}{N} \int_0^\infty dt e^{i\omega t} \text{tr} \left(\rho[\hat{O}(t), \hat{O}] \right), \quad (24)$$

with β being the inverse temperature.

The connection between QFI and multi-partite entanglement holds [40] for local operators \hat{O} with bounded spectrum. For instance, consider a scenario where \hat{O} is composed of a sum of one-body operators \hat{o}

$$\hat{O} = \sum_{j=1}^N \hat{o}_j, \quad (25)$$

with an associated spectral width

$$\Delta_o = o_{\max} - o_{\min}, \quad (26)$$

where o_{\min} and o_{\max} correspond to minimum and maximum eigenvalues of \hat{o} . Then the operator, \hat{O} is said to have a bounded spectrum if the spectral width Δ_o is finite. For such operators, the QFI is bounded from above for k -producible states,

$$F_Q[\rho_{k\text{-prod}}, \hat{O}] \leq \left\{ \left\lfloor \frac{N}{k} \right\rfloor k^2 + \left(N - \left\lfloor \frac{N}{k} \right\rfloor k \right)^2 \right\} \Delta_o^2. \quad (27)$$

In the special case when k is a divisor of N , this condition simplifies to

$$f_Q \leq k\Delta_o^2, \quad (28)$$

An assumption is made in situations when N is very large i.e. in the thermodynamic limit then every k is treated as a divisor of N . Thus, in the event the QFI density violates the bound above, we can say that underlying state has at least $(k+1)$ -partite entanglement i.e., has a minimum entanglement depth of $(k+1)$,

$$f_Q > k\Delta_o^2 \implies \rho \text{ is at-least } (k+1)\text{-partite entangled.} \quad (29)$$

In preparation for what's coming, we will work the following operator

$$\hat{O}(q) = \sum_r e^{iqr} \hat{S}^z(r), \quad (30)$$

where r is a discrete lattice site index and q is the discrete momentum. By using the fluctuation-dissipation theorem (FDT), the dissipative part of the dynamical susceptibility χ'' can be related to the dynamic structure factor $S^{zz}(q, \omega)$ [80],

$$\chi''(q, \beta, \omega) = \pi(1 - e^{-\beta\omega}) S^{zz}(q, \omega, \beta), \quad (31)$$

a quantity accessible in INS.

For temperature below some threshold value $T < T_Q$, it was shown [81] that the equal time structure factor, using it's connection to the QFI, can also be used as multi-partite entanglement witness,

$$4S^{zz}(q, \beta) > k \implies \rho \text{ is at-least } k\text{-partite entangled,} \quad (32)$$

where $S^{zz}(q, \beta)$ is the equal time structure factor

$$S^{zz}(q, \beta) = \int_{-\infty}^{\infty} d\omega S^{zz}(q, \omega, \beta). \quad (33)$$

Note that at zero temperature, for a pure state, the equal time structure factor is proportional to the QFI density

$$f_Q(q) = 4S^{zz}(q). \quad (34)$$

III. NOTATION

With many averages and sums being taken, we would like to bear out the notation here for ease of reading the

plots. To evaluate the disorder-average over M random realizations within an ensemble we consider

$$\bar{\Gamma} = \frac{1}{M} \sum_{m=0}^{M-1} \Gamma^{(m)}, \quad (35)$$

where Γ can correspond to some observable

$$\Gamma^{(m)} \equiv \langle \Gamma \rangle_m \quad (36)$$

or an entanglement measure discussed in Sec. II. For measures with explicit site dependence, we also perform an average over sites

$$\bar{\Gamma}_n = \frac{1}{MN} \sum_{i=0}^{N-1} \sum_{m=0}^{M-1} \Gamma_{ii+n}^{(m)}, \quad (37)$$

represents the disorder-averaged observable for the n -th neighbor of the N -site spin chain. For example Γ_{ij} can be thought to depict the two-point spin correlation or the pairwise concurrence.

IV. OVERVIEW OF HEISENBERG SPIN CHAINS

In this section we will briefly summarize necessary background pertaining to the Tomonaga Luttinger Liquid (TLL) and random singlet (RS) state in $d = 1$. In this article, by TLL we refer to the long length scale theory of the Heisenberg (i.e. XXX) spin chain characterized by the Luttinger parameter, $K = 1/2$ [82]. On the other hand, we interpret the strong disorder renormalization group (SDRG) [63] as the long length-scale theory of the RS state.

We consider the Heisenberg Hamiltonian with anti-ferromagnetic (AF) interactions

$$H = \sum_{i=0}^{N-1} J_i \mathbf{S}_i \cdot \mathbf{S}_{i+1}, \quad (38)$$

where J_i corresponds to the coupling strength between nearest neighbors, and \mathbf{S}_i are the usual $S = 1/2$ vector operator at site i .

The isotropic case corresponds to the scenario when all the couplings are equal i.e.,

$$J_i = J (> 0) \quad \forall i. \quad (39)$$

In this case, the model realizes a $SU(2)$ symmetric ground state, whose long wavelength behavior provides an example of a TLL, with correlation function [83, 84]

$$\lim_{|i-j| \rightarrow \infty} g_{ij}^{zz} \sim \frac{(-1)^{|i-j|} \sqrt{\log(|i-j|)}}{2\pi^{3/2} |i-j|^{\eta_{\text{TLL}}}}, \quad (40)$$

showcasing a power-law decay with exponent

$$\eta_{\text{TLL}} = 1. \quad (41)$$

specific to $K = 1/2$. We note that the logarithmic corrections in Eq. (40) arise due to the irrelevant operators that become marginal for the isotropic Hamiltonian [83, 84]

We now turn to the case where the couplings J_i in Eq. (38) are positive, and randomly drawn from some probability distribution $P(J)$. In this case one realizes a RS state whose long-wavelength is well characterized by the SDRG framework [63]. Disorder-averaged correlation functions decay algebraically

$$\lim_{|i-j| \rightarrow \infty} \bar{g}_{ij}^{zz} \sim \frac{(-1)^{|i-j|}}{|i-j|^{\eta_{\text{RS}}}}, \quad (42)$$

with exponent

$$\eta_{\text{RS}} = 2, \quad (43)$$

independent of the choice of $P(J)$. Recently, however, logarithmic corrections to the above disorder averaged correlations have also been reported [85].

V. SETTING UP THE PROBLEM

In this Section we make concrete our problem. Our goal here is to analyze what the previously introduced measures inform about the nature of entanglement of the TLL and RS states, respectively and whether one can use them in a meaningful way to distinguish between the two states. We investigate the antiferromagnetically interacting Heisenberg Hamiltonian in Eq. (38), with interactions drawn from a box distribution

$$P(J) = \begin{cases} \frac{1}{2\Delta}, & \text{if } J \in (1 - \Delta, 1 + \Delta] \\ 0, & \text{otherwise,} \end{cases} \quad (44)$$

where Δ parametrizes the strength of disorder. For our investigations, we set

$$\begin{aligned} \Delta &= 1 \text{ [disordered]}, \\ \Delta &= 0 \text{ [clean]}. \end{aligned} \quad (45)$$

We make use of exact diagonalization for our analysis and use the quantum typicality method for finite temperature investigations [71, 72]. Throughout our analysis we restrict ourselves to spin chains of even length with periodic boundary conditions. For $T = 0$ investigations we focused on $M = 1001$ disorder realizations for N ranging from 16 to 30. For $T \neq 0$, we consider $M = 200$ disorder realizations for $N = 16$ and 24. For $N = 20$, we consider $M = 100$ disorder realizations. In addition, we have taken into account 100 thermal pure quantum (TPQ) state samples for all three system sizes.

VI. ZERO TEMPERATURE RESULTS

In what follows we will discuss the entanglement structure of TLL and RS states as characterized by concurrence, RT and QFI at zero temperature.

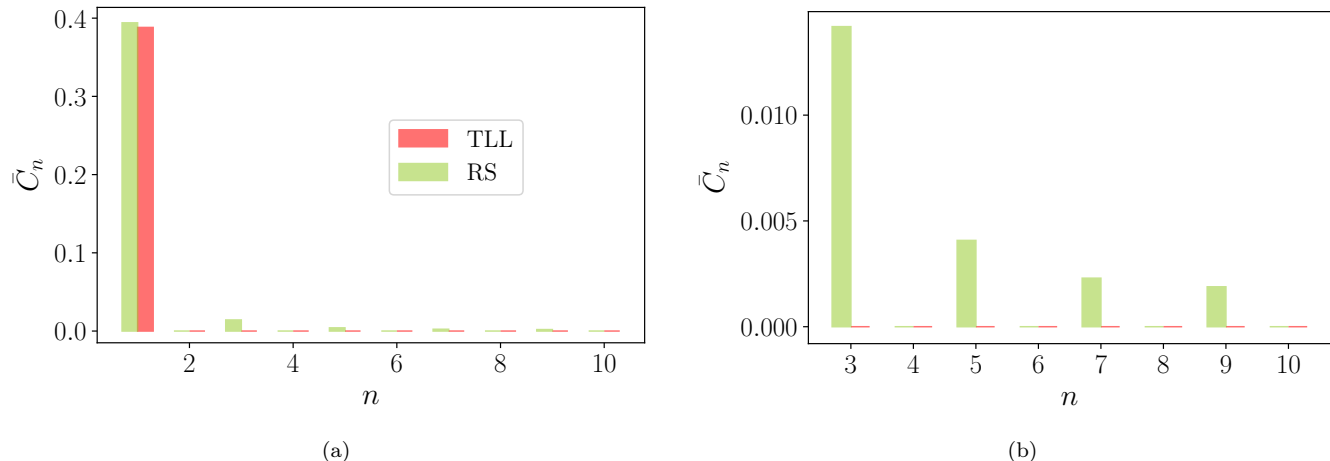


FIG. 1. Comparison of the nearest and beyond nearest neighbor concurrence distribution in Tomonaga Luttinger liquid (TLL) and random singlet (RS) state. (a) Concurrence distribution between neighbors n ranging from 1 to 10. (b) Concurrence distribution for $n > 2$ neighbors. Here the bars indicate the height of the data values. As evident, the distribution of concurrence is localized only amongst the nearest neighbors for the TLL state while it is spread to further neighbors in the RS state. The plots here were obtained for a $N = 30$ spin chain using Eq. (13) for the TLL, followed by an average of the sites. For the RS state, we evaluate Eq. (37) where Γ is concurrence. For ease of viewing, the error bars have been suppressed.

A. Nearest neighbor and beyond

We start by looking at the distribution of pairwise entanglement in the two states. In Fig. 1, we explore how the concurrence is distributed on the spin chain. For the RS state, we calculate the disorder-averaged concurrence i.e., we evaluate the g_{ij}^{zz} correlation function for each realization and then from it obtain the corresponding concurrence using Eq. (13). Thereafter we average over the concurrence per disorder realization as per Eq. (37). For the TLL, we evaluate the sum in Eq. (37) without the disorder-average. As evident in Fig. 1, the TLL only has nearest neighbor pairwise entanglement [86, 87] while the RS also has a finite contribution coming from further neighbors as can be seen in Fig. 2 for chosen disorder realizations. However, relative to the contribution from the nearest neighbors it is quite small and in fact from the point of view of INS probes, is not observable. We explain this later in Sec. VII A.

B. TLL and RS are multipartite entangled

To further understand the entanglement structure of these states next, we employ the multi-partite measures, i.e RT and QFI. We find that both the TLL and RS state show a finite multi-partite entanglement as seen through the RT Fig. 3 and QFI Fig. 4.

For the TLL, in Fig. 3, we observe the RT approaching

$$\bar{\tau}_3 = 0.701553, \quad (46)$$

it's value in the thermodynamic limit, calculated using Bethe Ansatz [87, 88].

On the other hand, for the RS state, the RT is fairly constant evidencing the existence of multi-partite entanglement. This is contrary to the SDRG picture, where the RS state is pictured as a tensor product of singlets spanning the chain, per disorder realization [63].

Accordingly, a straightforward implication of such a picture is that the RT should vanish for the RS state. However, for the system sizes that we can access, we do not observe such a vanishing behavior Fig. 3.

The multi-partite nature of the TLL [81] and RS is also predicted by the QFI. At the $q = \pi$, we observe that the TLL is at-least 6-partite entangled and that the RS state is at-least 4-partite entangled for the largest spin chain size ($N = 30$) we access. From Fig. 4 one can also see an increasing entanglement depth with system size both in the TLL and RS state at the $q = \pi$ point. This growth, however, is more pronounced in the TLL as compared to the RS state. The implication of such a result is that if one observes a multi-partite entanglement using QFI in an experiment, then one cannot simply rule out the RS state as one might have inferred from it's schematic picture.

In the thermodynamic limit, one expects that the QFI for the TLL to diverge logarithmically [89]. On the other hand, for the RS state, a complete suppression of QFI to a constant value is expected [85, 90].

VII. FINITE TEMPERATURE RESULTS

Having discussed the zero temperature entanglement structure of the two states, we move to explore the effects

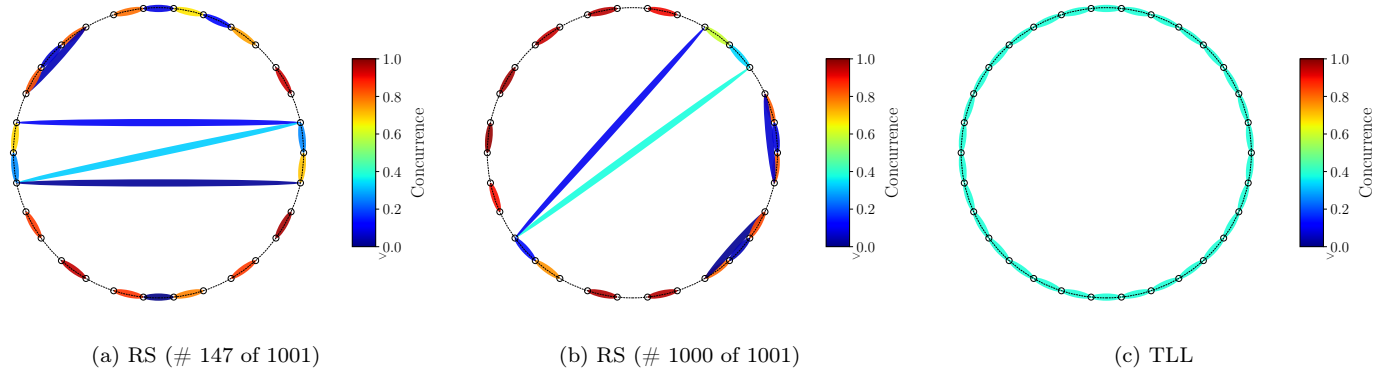


FIG. 2. Visually demonstrating the difference in the concurrence distribution between the random singlet (RS) and Tomonaga Luttinger liquid (TLL) state respectively. (a) Concurrence distribution of the 147th disorder realization. (b) Concurrence distribution of the 1000th disorder realization. (c) Concurrence distribution of the TLL. While TLL only has nearest neighbor concurrence, the RS state has a non-zero concurrence for odd neighbors at all length scales. The plots here were obtained for a $N = 30$ spin chain.

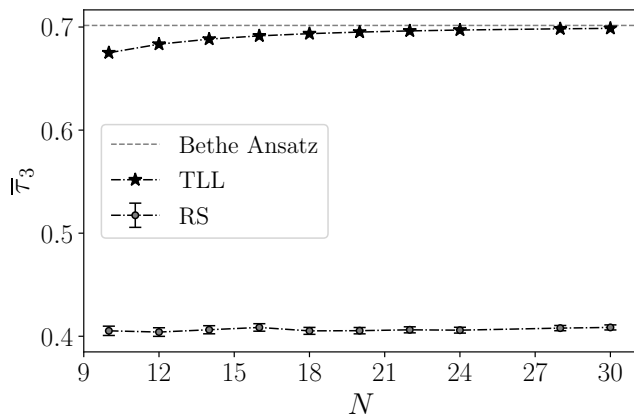


FIG. 3. Finite residual tangle (RT) indicating the existence of multi-partite entanglement in the Tomonaga Luttinger liquid (TLL) and random singlet (RS) state. RT of TLL is approaching close to its Bethe Ansatz value as N increases. For the RS, RT remains fairly constant.

of finite temperature on this structure. For the task at hand, we employ concurrence and the equal-time structure factor as entanglement witness based measures. In Sec. VII A, we discuss the importance of realizing what is being experimentally accessed and how it effects the way one performs the disorder-average in their analysis. In particular, we highlight the importance of knowing how to perform the disorder-average keeping in mind the observables accessible in an experiment. We point that this is especially crucial when one is trying to rule out disorder induced states by using certain entanglement measures. Following which, in Sec. VII C, we find that the low-temperature growth of entanglement witness based measure turns out to be very useful to characterize these states.

A. The order of disorder-average matters for concurrence

If one goes by our previous results for concurrence then one expects to see beyond nearest neighbor 2-partite entanglement in the RS state. Does this imply that if experimentally we do not observe further nearest neighbor concurrence can we rule out the presence of a disorder induced state? On the practical side, can the further nearest neighbor entanglement even be observed in INS? Unfortunately, the answer to both these questions turns out to be negative. Typically, in experimental situations such as in INS, we access disorder-averaged spin correlations. What this means is that when characterizing entanglement from spin correlation for example, one does not access the entanglement per disorder realization. While this distinction might feel academic, for measures like concurrence, the order of how one performs to disorder-average becomes important if one is comparing a theoretical model against the experimental predictions.

To begin with, let's look at the finite temperature behavior of concurrence with the way we have been evaluating it as explained in Sec. VI A. In Fig. 5, we find that upto some threshold temperatures the RS state has finite pairwise entanglement from further neighbors whereas the TLL state has only nearest neighbor pairwise contribution consistent with what we saw before.

On the other hand, we can also evaluate the disorder-average of the spin correlations first and then evaluate the concurrence as below

$$C_{ij} = 2 \max \left\{ 0, 2|\bar{g}_{ij}^{zz}| - \left| \frac{1}{4} + \bar{g}_{ij}^{zz} \right| \right\}, \quad (47)$$

where \bar{g}_{ij}^{zz} is the disorder-averaged spin correlation function evaluated as per Eq. (35). From the experimental perspective, it is this concurrence that would be accessed.

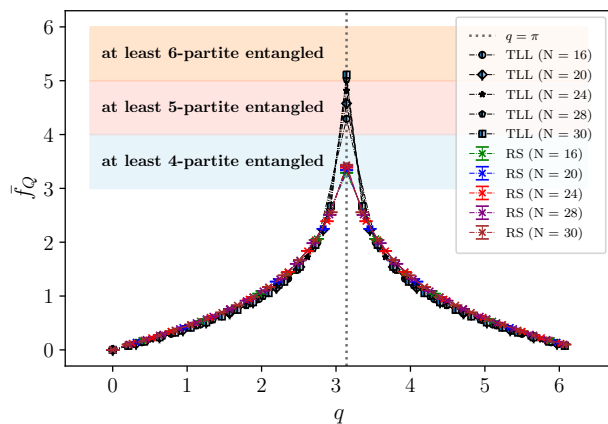
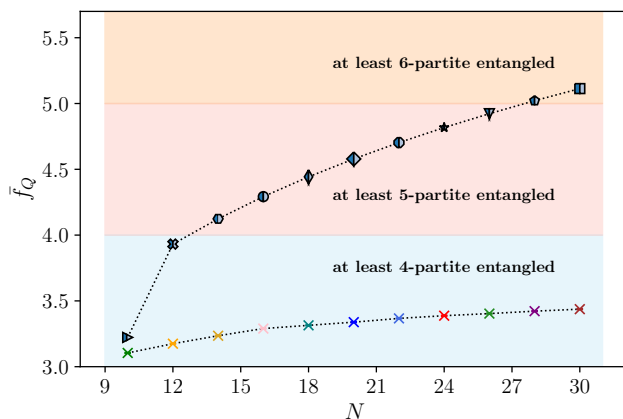
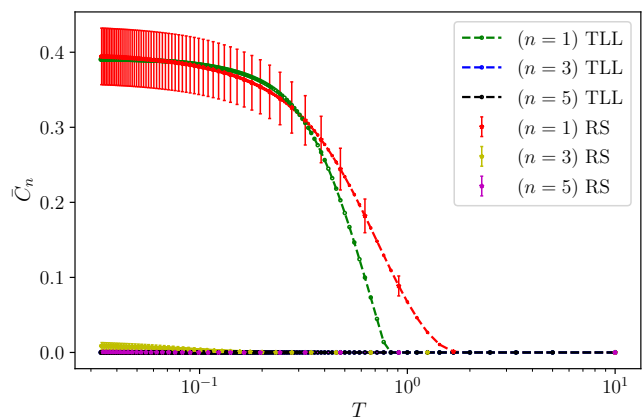
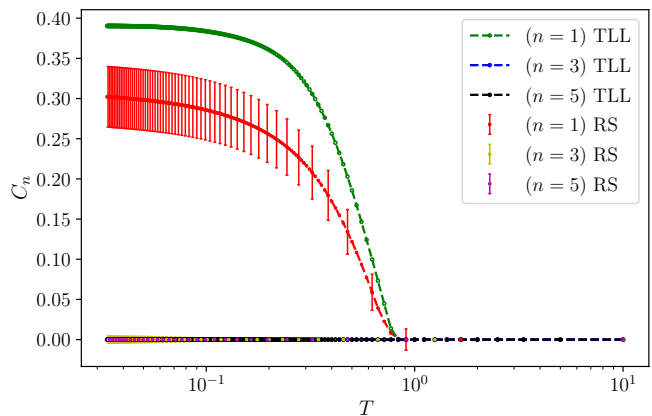
(a) QFI density vs q (b) Scaling of QFI density at $q = \pi$

FIG. 4. Observing the growth of entanglement depth at the $q = \pi$ point in Tomonga Luttinger liquid (TLL) and random singlet (RS) state. (a) Quantum Fisher Information (QFI) density for TLL and RS state plotted as function of q for $N = 16, 20, 24, 28, 30$. (b) QFI density plotted as function of N at $q = \pi$ point for TLL and RS state. The rate of growth of entanglement depth is suppressed in the RS state. Here we observe the TLL state to be at-least 6-partite entangled while the RS is at least 4 partite entangled.

In Fig. 6, we perform this and find that RS has only nearest neighbor 2-partite entanglement just like the TLL. We do not observe any finite beyond nearest neighbor concurrence as one might have expected. What this means is that experimentally one would not be able to observe beyond nearest neighbor pairwise entanglement if they access disorder-averaged spin correlations. Thus ruling out the RS state by looking at the 2-tangle or concurrence and observing no beyond nearest neighbor 2-partite entanglement is incorrect. We also observe in Fig. 5b that the nearest neighbor concurrence vanishes at the same temperature for both the TLL and RS state.



(a) Disorder-averaged Concurrence at finite temperature



(b) Concurrence from disorder-averaged spin correlations

FIG. 5. Demonstrating how the order of disorder-average affects the concurrence distribution in the random singlet (RS) state. (a) Disorder-averaged concurrence observed for 1st, 3rd and 5th neighbors as function of temperature for $N = 20$. (b) Concurrence, obtained from disorder-averaged spin correlations, observed for the 1st, 3rd and 5th neighbors as a function of temperature. For (a), concurrence is evaluated using Eq. (13) for every disorder realization and then averaged. On the other hand, for (b), concurrence is evaluated using Eq. (47). in which case the pairwise entanglement distribution of the RS state mimics the Tomonga Luttinger liquid (TLL) state i.e., becomes nearest neighbored. To help read the plots some of the error bars coming from disorder averages have been suppressed.

B. The low-temperature behavior of concurrence contains central charge

The low-energy behavior of TLL can be described by a conformal field theory with a central charge, $c_{\text{TLL}} = 1$ [89]. By noting that the nearest neighbor concurrence for a TLL can be related to internal energy, one can easily obtain the central charge as follows. The key is to realize that the nearest neighbor concurrence can be related to

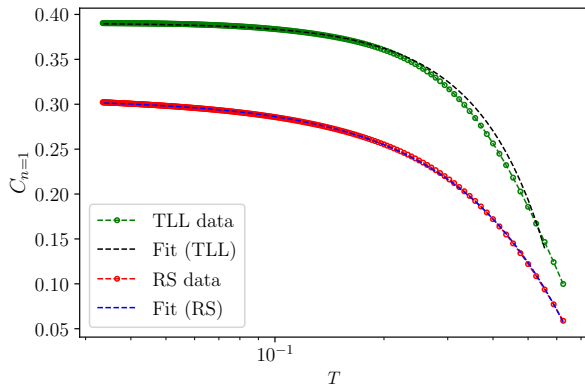


FIG. 6. Extracting central charge information from the low-temperature behavior of concurrence for the Tomonga Luttinger liquid (TLL) and random singlet (RS) state respectively. The plots here are evaluated for $N = 20$ spin chain. For the TLL state, we make use of Eq. (48) and Eq. (49) to fit the observed low-temperature behavior. For the RS state, we make use of Eq. (48) and Eq. (52) for the observed low-temperature behavior. Note that here we are evaluating the concurrence from disorder-averaged spin correlations [Eq. (47)] as one would access in experiments like inelastic Neutron scattering (INS). For ease of viewing, the error bars have been suppressed.

the internal energy as follows.

$$C_1 = \max\{0, 2|u(T)| - 0.5\}, \quad (48)$$

where

$$u(T) = u(0) + cT^2 \left(\frac{1}{3} + \frac{3 + \log(\pi/T)}{8 \log(\pi/T)^4} \right), \quad (49)$$

is the low-temperature behavior of the internal energy [91] and c is the central charge.

We put this to test in Fig. 6 and find a good agreement with the our fit

$$u(0) \approx -0.445, \quad c_{\text{TLL}} \approx 1.01 \quad (50)$$

On the other hand, it has been shown that the RS state is characterized by an effective central charge [92]

$$c_{\text{RS}} = c_{\text{TLL}} \ln 2. \quad (51)$$

We conjecture that it is possible to access this information from the concurrence of the RS state where we employ the disorder-average that is experimentally relevant. We find the following ansatz fits very well with the observed low-temperature behavior for the RS state

$$u(T) = u(0) + \frac{c_{\text{eff}} T^d}{3}, \quad (52)$$

where d is a fit parameter and

$$c_{\text{eff}} = c \log(2), \quad (53)$$

is what we interpret as the effective central charge. In Fig. 6 we obtain

$$u(0) \approx -0.403, \quad c_{\text{eff}} \approx 0.71, \quad d \approx 1.39, \quad (54)$$

where the parameter $u(0)$ is size-dependent, and we find c to be very close to c_{TLL} .

C. The low-temperature growth of multi-partite entanglement is a useful probe

We saw that the zero temperature QFI, Fig. 4, predicts both the TLL and RS state to be multi-partite entangled. Thus, stating whether a state is m -partite or some other is l -partite is not a very useful probe if we want to distinguish them experimentally. Instead, we propose to investigate the low-temperature behavior of multi-partite entanglement witness measures. We employ the equal time structure factor for this task. As evident in Figs. 7, the growth of entanglement at low-temperatures is qualitatively quite different. For the TLL, the low-temperature scaling behavior is well known [93]

$$4S^{zz}(q = \pi, \beta) = D \log(T_o \beta)^{3/2}. \quad (55)$$

We confirm that Fig. 7b

$$D \approx 0.46, \quad T_o \approx 10, \quad (56)$$

upto a range of temperatures our results match very well with Eq. (55), however at lower temperatures, we do observe finite size effects for the different spin chain sizes we explore.

On the other hand, we find the growth of entanglement to be quite slow in our disorder induced state. We propose the following empirical behavior,

$$4S^{zz}(q = \pi, \beta) = a\beta^b + d, \quad (57)$$

which we found for

$$a \approx -1.5, \quad b \approx -0.6, \quad d \approx 3.1 \quad (58)$$

to describe our data Fig. 7c very nicely. These parameter values are system size and disorder strength of disorder dependent, however.

VIII. DISCUSSION

A. Qualitative pictures at long length scales can be misleading

We highlight the need to be careful with qualitative pictures when it comes to ruling out RS states. Within the SDRG approach, the RS state is pictured a tensor product of pairwise entangled sites per disorder realization Fig. 8a. Consequently, this approach rules out the

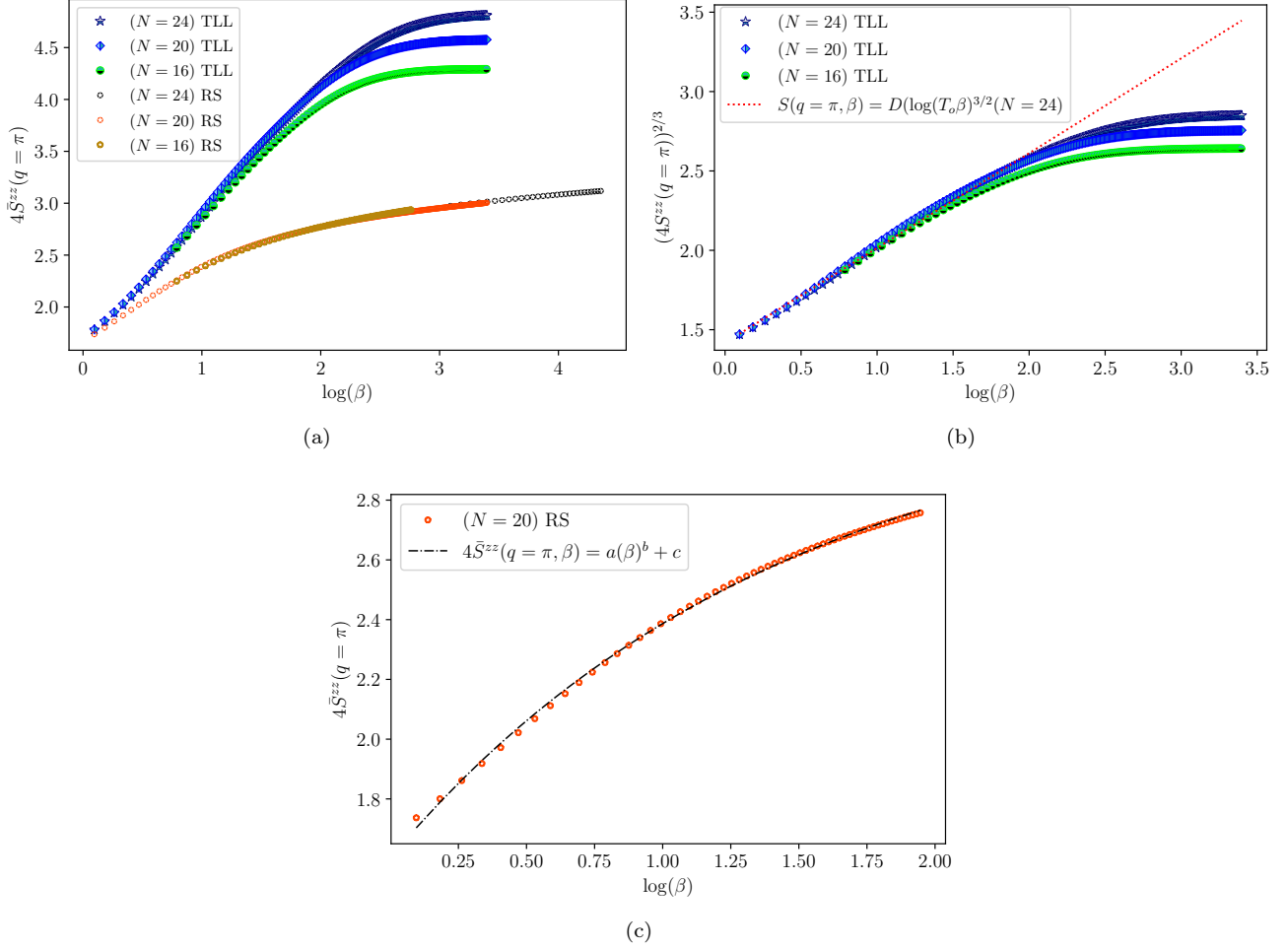


FIG. 7. Comparison of the low-temperature behavior of the equal time structure factor for the Tomonga Luttinger liquid (TLL) and random singlet (RS) state. (a) Equal time structure factor of both the TLL and RS states observed as function of $\log(\beta)$ for $N = 16, 20, 24$ chains. (b) Testing the low-temperature behavior of equal time structure factor for the TLL against the analytic prediction Eq. (55). (c) Testing the low-temperature behavior of equal time structure factor for the RS against the ansatz Eq. (57) for $N = 20$ spin chain. The fitting parameters are given in Eq. (56) and Eq. (58). The fits were checked within a fixed interval $0.09 < \log(\beta) < 1.9$ for both the TLL and RS state. This choice was made owing to the finite size effects in the TLL state for temperatures below the lower bound. For ease of viewing, the error bars have been suppressed.

existence of any entanglement beyond the pairwise setting. On the other hand, both RT Fig. 3 and QFI Fig. 4, point to the RS state to be multi-partite entangled. In particular, we observed that at $q = \pi$, the QFI density predicts the RS state to be at-least 4-partite entangled for the largest spin chain size $N = 30$ that was accessed. Clearly, there is a paradox here.

B. Multi-partite entanglement localization and understanding RS ‘state’

What is the reason for this apparent contradiction? The confusion stems from what one means by the ‘state’ here. Whether one means the critical ground state of the Hamiltonian having information about all the length

scales or only the effective state that characterizes the long wavelength physics. These are not the same, especially with regards to entanglement.

The SDRG framework provides an extremely good description of the the long-wavelength behavior of a disordered spin chain [94, 95]. The success of a picture based on a product of singlets implies that the entanglement needed to describe long-wavelength physics is at most 2-partite. However this long-wavelength picture, in which correlations are controlled by the strong-disorder fixed point, should be understood to apply beyond a crossover length, L_c [94]. This crossover can be observed in Fig. 4a, as a momentum

$$q_c = \pi - \frac{2\pi}{L_c}, \quad (59)$$

above which the RS state and the TLL are practically

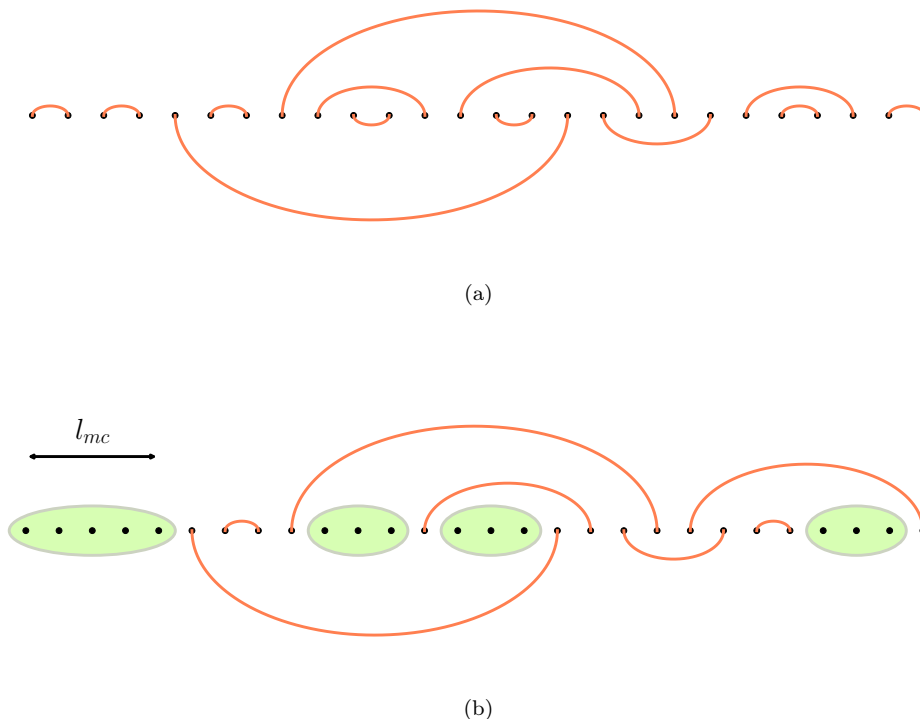


FIG. 8. An illustration of the ground state of the disordered spin chain. (a) The schematic picture of the random singlet (RS) state, as described within the strong disorder renormalization group (SDRG), where pairs of entangled sites are connected by orange colored arcs. (b) Schematic picture of the RS state predicted from our results, where multi-partite clusters (mc) are represented by green shaded ovals of size l_{mc} alongside pairwise entangled sites connected by orange colored arcs. These mc are localized to distances below the crossover length L_c .

indistinguishable.

At distances shorter than L_c , spins may be entangled in clusters and exhibit multipartite entanglement, as illustrated in Fig. 8b. However for distances $\gg L_c$, these multi-partite clusters become irrelevant, and entanglement is at most 2-partite. It follows that one should interpret the effective RS state obtained from SDRG as being defined above L_c . At short length scales, the multipartite entanglement plays a role, as witnessed by the QFI density [Fig. 4a]. We can understand this as the localization of the multi-partite entanglement.

We can turn this observation into a bound on QFI density. If the RS state, as understood within the SDRG, is at most 2-partite entangled, this places a limit on the entanglement contributed by long lengthscales. We therefore expect

$$\bar{f}_Q(q = \pi) - \bar{f}_Q(q = q_c) \leq 2, \quad (60)$$

A violation of this inequality would rule out the RS state.

To summarize the above discussion the ground state of a disordered spin chain, the ‘true’ RS state is a multipartite entangled state. While the multi-partite entanglement is not relevant to understand the behavior it does

exist. This multi-partiteness is resultant from contributions below the crossover length i.e., from the short range physics.

C. Infinite disorder and Thermodynamic limit.

Up until now we focussed on a setting where we considered a box distribution as specified in Eq. (44) with $\Delta = 1.0$. How does the understanding change for some other distribution? To make this question more concrete let us consider the following family of distributions

$$P(J; \delta) = \begin{cases} A\delta^{-1}J^{\delta-1} & \text{for } 0 \leq J < J_{max} \\ 0 & \text{otherwise,} \end{cases} \quad (61)$$

where

$$A = 1/J_{max}^{1/\delta}. \quad (62)$$

Note that for $\delta = 1$ and $J_{max} = 2$ we recover the boxed distribution Eq. (44). In the limit $\delta \rightarrow \infty$, one obtains the infinite randomness fixed point (IRFP) of the SDRG method.

For starters, an increasing δ reduces the observed entanglement depth at the $q = \pi$ point as seen in Fig. 9.

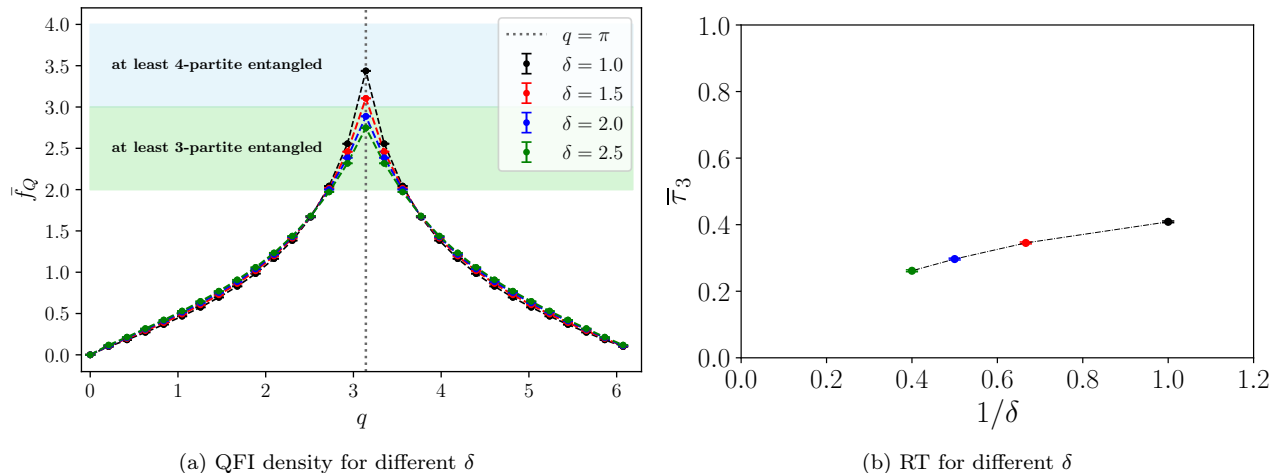


FIG. 9. Observing the decreasing entanglement depth with increasing δ in the random singlet (RS) state. (a) Quantum Fisher information (QFI) density as function of q for $\delta = 1.0, 1.5, 2.0, 2.5$ in a $N = 30$ spin chain. (b) Residual tangle (RT) as a function of $1/\delta$ for $N = 30$ chain, where the line is used as a guide. While an increasing δ reduces the entanglement depth, for $\delta = 2.5$ and $N = 30$ spin chain the QFI density at the $q = \pi$ still detects a multi-partite entangled RS state.

This in turn moves the crossover momentum q_c Eq. (59) further away from π . Thus, Eq. (60) remains valid for increasing δ as well. The disorder parameter δ controls the crossover length and which consequently bounds the maximum length of the multi-partite cluster, l_{mc}

$$l_{mc} \leq L_c, \quad (63)$$

such that the role of these clusters become increasingly negligible above the crossover length. What does one expect in the thermodynamic limit? At least, for a finite δ , say below $\delta \leq \delta^* = 2.5$, from our results, we do expect to observe an entanglement depth greater than 2

$$\lim_{\delta \rightarrow \delta^*} \lim_{N \rightarrow \infty} f_Q(q = \pi) = C_* > 2, \quad (64)$$

where C_* is some constant. For real materials, a finite δ would already imply an entanglement depth larger than two. For instance, in [96], it was reported that $\text{Ba}_5\text{CuIr}_3\text{O}_{12}$ single crystals can characterize a RS state with a $\delta \approx 2.5$.

D. Experimentally ruling out RS states is a subtle business

The RS state, by which we mean the ground state of the disordered spin chain, is not a simple a tensor product of singlets. This could have been inferred from the results in [90, 97], in hindsight. While the 2-partite entanglement of this state may indeed be the relevant entanglement setting to understand the effects of disorder, it does also have a multi-partite contribution from length scales below the crossover length. Even though the multi-partite nature of the state may not be relevant to understand the effects of disorder at long length

scales, these contributions do not simply disappear either. Consequently, ruling out RS states under the assumption that it has only 2-partite entanglement is incorrect. Furthermore, we showed how one might be misled into ruling out RS state by the absence of any concurrence beyond the nearest neighbors. One might incorrectly conclude the absence of long range singlets from such an observation.

Convex roof measures like concurrence depend quite a lot on the way the disorder-average is performed. This is due to the presence of the ‘max’ function in the definition Eq. (10). The operation of averaging over disorder realizations does not commute with the max operation. Whether one takes the disorder-average inside the max function, or outside it, the end results are completely different. Why is this important? For quenched disordered systems, the spin correlations are already disorder-averaged. Thus if one were to access spin correlations from experiments like INS and from those tried evaluated concurrence using Eq. (47) then one would observe Fig. 5b as opposed to Fig. 5a. The former corresponds to the case when concurrence has been evaluated from disorder-averaged spin correlations and the latter is the one where we evaluate concurrence for each disorder realization and then average it. In the former case, the RS state shows no further neighbor concurrence, essentially mimicking the TLL state at the 2-partite level Fig. 2c. In [57], the authors incorrectly ruled out RS states by observing vanishing concurrence and multi-partite entanglement using QFI. However, both of these observations cannot rule out the RS state as shown in Sec. VIB and VII A. This point will be discussed further in a follow-up work [98].

E. What can be useful experimentally?

For 1d critical states, the low-temperature behavior of concurrence can access central charge information. In particular, the nearest neighbor concurrence of an $SU(2)$ symmetric ground state can be related to the internal energy, and this allowed us to extract the central charge of the TLL state. On the other hand, for RS state, while the order of disorder-average effects how concurrence is distributed among the sites, the universal information about the state should still be accessible if it is contained within the 2-partite entanglement. This universal information is the effective central charge. Since experimentally, the concurrence distribution for the RS state can be nearest-neighbored just as the TLL, we thought that perhaps one might be able to access the effective central charge for the RS state. This is based on the assumption that there exists a form of generalized c-theorem for the RS state[92]. This is what we put to test in Fig. 6 and see some positive indications. However, we admit that this is conjectural at best.

On the other hand, multi-partite entanglement witnesses like the QFI or the equal time structure factor are invaluable markers for not only identifying the existence of multi-partite entanglement but also how disorder affects their growth. We saw this by the marked difference in the low-temperature behavior of the equal time structure factor in the TLL and RS state. This behavior can be experimentally useful in identifying the role of disorder in spin chains.

F. Limitations to detection of multi-partite entanglement

Measures like QFI, when accessed via the dynamic structure factor, can only detect multi-partite entanglement if the underlying state shows correlations peaked around specific \mathbf{q} points. Due to the sum rule, this structure constraints the visibility of multi-partite entanglement detection at other \mathbf{q} points. However, such peaked structure factors are not universal. For instance, in Kitaev and Kagome QSLs, there are no special \mathbf{q} points with sharp features [99–101]. Therefore, multi-partite entanglement cannot be accessed using INS in these cases. This does not imply the absence of multi-partite entanglement in these states, rather, it suggests that the multi-partite entanglement could be spread among non-local correlations, rendering the operator used to access this information insufficient.

IX. CONCLUSIONS

While there are no perfectly clean samples in nature, none are infinitely disordered either. In this work, we set

out to understand how one can experimentally access the affects of disorder on the entanglement of ground states within condensed matter systems. We utilized the quantum spin chain as a representative example to investigate the impact of bond disorder. In this setting, we focussed on distinguishing between Tomonaga-Luttinger liquid (TLL) and random singlet (RS) states through experimentally accessible entanglement measures, like concurrence, residual-tangle (RT) and quantum fisher information (QFI).

We saw that both the TLL and RS states are multi-partite entangled. For the TLL, the observed multi-partite entanglement is a consequence of the uninhibited growth of correlations. On the other hand, such correlations are completely suppressed for the RS state. Consequently, the observation of multi-partite entanglement in the RS state is consequence of the localization of multi-partite clusters upto a crossover lengthscale. Above this regime, the relevant entanglement might indeed be 2-partite, consistent within the framework of strong disorder renormalization group (SDRG). To better characterize the effect of disorder, we introduced the inequality Eq. (60) which we found is also in agreement for the larger system sizes that were accessed in [90, 97].

For quenched disorder, the order of average matters for convex roof measures. In particular, the distribution of pairwise entanglement, as characterized by concurrence, depends on how one performs the average. For the RS state, this distribution can transform from being shared between distant sites Fig. 5a to only among nearest neighbors Fig. 5b, as is the case in TLL. Since in INS one would access disorder-averaged correlations, it is the latter that one would observe rather than the former.

For the TLL, it is well established that it can be described by a conformal field theory. We leveraged this connection to extract the associated central charge from the low-temperature behavior of concurrence. Conversely, for the RS state, we extracted the effective central charge from the low-temperature behavior of concurrence by employing disorder averaging accessible in experiments. This relies on appreciating that the order of disorder averaging alters the distribution of pairwise entanglement while preserving the universal information encoded within it. However, the existence of an effective central charge for the RS state remains conjectural, based on the assumption of a generalized c-theorem [92].

From the experimental point of view, a more robust characteristic is to examine the low-temperature behavior of multi-partite entanglement witnesses like quantum Fisher information (QFI) or the equal time structure factor. We made use of the equal time structure-factor to show a marked difference in the rate of growth of

multi-partite entanglement within the two states Fig. 7a. This scaling provides a clear distinction between the TLL and RS states, which can be observed experimentally.

In the end, we would like to conclude, by pointing out that, in general some caution should be maintained especially when ruling out disorder-induced states using measures based on witnesses. However, when used carefully, these can provide important information about quantum spin systems in the presence of disorder.

ACKNOWLEDGEMENTS

This work is supported by the Theory of Quantum Matter Unit of the Okinawa Institute of Science and

Technology Graduate University (OIST). We would like to thank Allen Scheie, Alan Tennant, and Francis Pratt for sparking our interest in this problem. We also thank Matthias Gohlke, Geet Rakala, and Pranay Patil for their helpful suggestions and discussions. The calculations done here were performed using HΦ [102]. This study is also supported by JSPS KAKENHI Grant Numbers 21K03477, 22H05266 and 24H00974. Majority of the numerical calculations were performed using the Core Facilities of the Scientific Computing and Data Analysis section at OIST. Some parts were also done using the facilities of the Supercomputing Center, at ISSP, University of Tokyo.

-
- [1] Y. Shimizu, K. Miyagawa, K. Kanoda, M. Maesato, and G. Saito, Spin liquid state in an organic mott insulator with a triangular lattice, *Phys. Rev. Lett.* **91**, 107001 (2003).
- [2] Y. Kurosaki, Y. Shimizu, K. Miyagawa, K. Kanoda, and G. Saito, Mott Transition from a Spin Liquid to a Fermi Liquid in the Spin-Frustrated Organic Conductor κ -(ET)₂Cu₂(CN)₃, *Phys. Rev. Lett.* **95**, 177001 (2005).
- [3] S. Yamashita, Y. Nakazawa, M. Oguni, Y. Oshima, H. Nojiri, Y. Shimizu, K. Miyagawa, and K. Kanoda, Thermodynamic properties of a spin-1/2 spin-liquid state in a κ -type organic salt, *Nature Physics* **4**, 459 (2008).
- [4] M. Yamashita, N. Nakata, Y. Kasahara, T. Sasaki, N. Yoneyama, N. Kobayashi, S. Fujimoto, T. Shibauchi, and Y. Matsuda, Thermal-transport measurements in a quantum spin-liquid state of the frustrated triangular magnet κ -(BEDT-TTF)₂Cu₂(CN)₃, *Nature Physics* **5**, 44 (2009).
- [5] F. Pratt, P. Baker, S. Blundell, T. Lancaster, S. Ohira-Kawamura, C. Baines, Y. Shimizu, K. Kanoda, I. Watanabe, and G. Saito, Magnetic and non-magnetic phases of a quantum spin liquid, *Nature* **471**, 612 (2011).
- [6] K. Watanabe, H. Kawamura, H. Nakano, and T. Sakai, Quantum spin-liquid behavior in the spin-1/2 random heisenberg antiferromagnet on the triangular lattice, *Journal of the Physical Society of Japan* **83**, 034714 (2014).
- [7] T. Shimokawa, K. Watanabe, and H. Kawamura, Static and dynamical spin correlations of the $S = \frac{1}{2}$ random-bond antiferromagnetic Heisenberg model on the triangular and kagome lattices, *Phys. Rev. B* **92**, 134407 (2015).
- [8] H.-Q. Wu, S.-S. Gong, and D. N. Sheng, Randomness-induced spin-liquid-like phase in the spin- $\frac{1}{2}$ $J_1 - J_2$ triangular heisenberg model, *Phys. Rev. B* **99**, 085141 (2019).
- [9] M. P. Shores, E. A. Nytko, B. M. Bartlett, and D. G. Nocera, A structurally perfect $s = 1/2$ kagome antiferromagnet, *Journal of the american chemical society* **127**, 13462 (2005).
- [10] J. S. Helton, K. Matan, M. P. Shores, E. A. Nytko, B. M. Bartlett, Y. Yoshida, Y. Takano, A. Suslov, Y. Qiu, J.-H. Chung, D. G. Nocera, and Y. S. Lee, Spin Dynamics of the Spin-1/2 Kagome Lattice Antiferromagnet ZnCu₃(OH)₆Cl₂, *Phys. Rev. Lett.* **98**, 107204 (2007).
- [11] T.-H. Han, J. S. Helton, S. Chu, D. G. Nocera, J. A. Rodriguez-Rivera, C. Broholm, and Y. S. Lee, Fractionalized excitations in the spin-liquid state of a kagome-lattice antiferromagnet, *Nature* **492**, 406 (2012).
- [12] R. R. P. Singh, Valence Bond Glass Phase in Dilute Kagome Antiferromagnets, *Phys. Rev. Lett.* **104**, 177203 (2010).
- [13] H. Kawamura, K. Watanabe, and T. Shimokawa, Quantum spin-liquid behavior in the spin-1/2 random-bond Heisenberg antiferromagnet on the kagome lattice, *Journal of the Physical Society of Japan* **83**, 103704 (2014).
- [14] M. Fu, T. Imai, T.-H. Han, and Y. S. Lee, Evidence for a gapped spin-liquid ground state in a kagome heisenberg antiferromagnet, *Science* **350**, 655 (2015).
- [15] H. Kawamura and K. Uematsu, Nature of the randomness-induced quantum spin liquids in two dimensions, *Journal of Physics: Condensed Matter* **31**, 504003 (2019), arXiv:1907.06176.
- [16] P. Khuntia, M. Velazquez, Q. Barthélemy, F. Bert, E. Kermarrec, A. Legros, B. Bernu, L. Messio, A. Zorko, and P. Mendels, Gapless ground state in the archetypal quantum kagome antiferromagnet ZnCu₃(OH)₆Cl₂, *Nature Physics* **16**, 469 (2020).
- [17] J. Wang, W. Yuan, P. M. Singer, R. W. Smaha, W. He, J. Wen, Y. S. Lee, and T. Imai, Emergence of spin singlets with inhomogeneous gaps in the kagome lattice Heisenberg antiferromagnets Zn-barlowite and herbertsmithite, *Nature Physics* **17**, 1109 (2021).
- [18] Q. Barthélemy, A. Demuer, C. Marcenat, T. Klein, B. Bernu, L. Messio, M. Velázquez, E. Kermarrec, F. Bert, and P. Mendels, Specific heat of the kagome antiferromagnet herbertsmithite in high magnetic fields, *Phys. Rev. X* **12**, 011014 (2022).
- [19] Y. Li, H. Liao, Z. Zhang, S. Li, F. Jin, L. Ling, L. Zhang, Y. Zou, L. Pi, Z. Yang, *et al.*, Gapless quantum spin liquid ground state in the two-dimensional spin-1/2 tri-

- angular antiferromagnet YbMgGaO_4 , *Scientific reports* **5**, 16419 (2015).
- [20] Z. Zhu, P. A. Maksimov, S. R. White, and A. L. Chernyshev, Disorder-Induced Mimicry of a Spin Liquid in YbMgGaO_4 , *Phys. Rev. Lett.* **119**, 157201 (2017).
- [21] J. A. Paddison, M. Daum, Z. Dun, G. Ehlers, Y. Liu, M. B. Stone, H. Zhou, and M. Mourigal, Continuous excitations of the triangular-lattice quantum spin liquid YbMgGaO_4 , *Nature Physics* **13**, 117 (2017).
- [22] I. Kimchi, A. Nahum, and T. Senthil, Valence Bonds in Random Quantum Magnets: Theory and Application to YbMgGaO_4 , *Phys. Rev. X* **8**, 031028 (2018).
- [23] K. Kitagawa, T. Takayama, Y. Matsumoto, A. Kato, R. Takano, Y. Kishimoto, S. Bette, R. Dinnebier, G. Jackeli, and H. Takagi, A spin-orbital-entangled quantum liquid on a honeycomb lattice, *Nature* **554**, 341 (2018).
- [24] J. Knolle, R. Moessner, and N. B. Perkins, Bond-Disordered Spin Liquid and the Honeycomb Iridate $\text{H}_3\text{LiIr}_2\text{O}_6$: Abundant Low-Energy Density of States from Random Majorana Hopping, *Phys. Rev. Lett.* **122**, 047202 (2019).
- [25] C. Lee, S. Lee, Y. Choi, C. Wang, H. Luetkens, T. Shiroka, Z. Jang, Y.-G. Yoon, and K.-Y. Choi, Coexistence of random singlets and disordered Kitaev spin liquid in $\text{H}_3\text{LiIr}_2\text{O}_6$, *Phys. Rev. B* **107**, 014424 (2023).
- [26] C. Broholm, R. J. Cava, S. A. Kivelson, D. G. Nocera, M. R. Norman, and T. Senthil, Quantum spin liquids, *Science* **367**, eaay0668 (2020), <https://www.science.org/doi/pdf/10.1126/science.aay0668>.
- [27] R. Islam, R. Ma, P. M. Preiss, M. Eric Tai, A. Lukin, M. Rispoli, and M. Greiner, Measuring entanglement entropy in a quantum many-body system, *Nature* **528**, 77 (2015).
- [28] A. M. Kaufman, M. E. Tai, A. Lukin, M. Rispoli, R. Schittko, P. M. Preiss, and M. Greiner, Quantum thermalization through entanglement in an isolated many-body system, *Science* **353**, 794 (2016).
- [29] M. Wieśniak, V. Vedral, and Āaslav Brukner, Magnetic susceptibility as a macroscopic entanglement witness, *New Journal of Physics* **7**, 258 (2005).
- [30] Brukner, Ā and Vedral, Vlatko and Zeilinger, Anton, Crucial role of quantum entanglement in bulk properties of solids, *Phys. Rev. A* **73**, 012110 (2006).
- [31] T. G. Rappoport, L. Ghivelder, J. C. Fernandes, R. B. Guimarāes, and M. A. Continentino, Experimental observation of quantum entanglement in low-dimensional spin systems, *Phys. Rev. B* **75**, 054422 (2007).
- [32] A. M. Souza, M. S. Reis, D. O. Soares-Pinto, I. S. Oliveira, and R. S. Sarthour, Experimental determination of thermal entanglement in spin clusters using magnetic susceptibility measurements, *Phys. Rev. B* **77**, 104402 (2008).
- [33] A. M. Souza, D. O. Soares-Pinto, R. S. Sarthour, I. S. Oliveira, M. S. Reis, P. Brandāo, and A. M. dos Santos, Entanglement and bell's inequality violation above room temperature in metal carboxylates, *Phys. Rev. B* **79**, 054408 (2009).
- [34] D. Soares-Pinto, A. Souza, R. Sarthour, I. Oliveira, M. Reis, P. Brandao, J. Rocha, and A. Dos Santos, Entanglement temperature in molecular magnets composed of s-spin dimers, *Europhysics Letters* **87**, 40008 (2009).
- [35] R. Horodecki, P. Horodecki, M. Horodecki, and K. Horodecki, Quantum entanglement, *Reviews of Modern Physics* **81**, 865 (2009).
- [36] O. Gūhne and G. Tóth, Entanglement detection, *Physics Reports* **474**, 1 (2009).
- [37] A. Candini, G. Lorusso, F. Troiani, A. Ghirri, S. Carretta, P. Santini, G. Amoretti, C. Muryn, F. Tuna, G. Timco, E. J. L. McInnes, R. E. P. Winpenny, W. Wernsdorfer, and M. Affronte, Entanglement in Supramolecular Spin Systems of Two Weakly Coupled Antiferromagnetic Rings (Purple- Cr_7Ni), *Phys. Rev. Lett.* **104**, 037203 (2010).
- [38] M. A. Yurishchev, Quantum discord in spin-cluster materials, *Phys. Rev. B* **84**, 024418 (2011).
- [39] M. S. Reis, S. Soriano, A. M. dos Santos, B. C. Sales, D. Soares-Pinto, and P. Brandao, Evidence for entanglement at high temperatures in an engineered molecular magnet, *Europhysics Letters* **100**, 50001 (2012).
- [40] P. Hyllus, W. Laskowski, R. Krischek, C. Schwemmer, W. Wiczeorek, H. Weinfurter, L. Pezzé, and A. Smerzi, Fisher information and multiparticle entanglement, *Phys. Rev. A* **85**, 022321 (2012).
- [41] D. Das, H. Singh, T. Chakraborty, R. K. Gopal, and C. Mitra, Experimental detection of quantum information sharing and its quantification in quantum spin systems, *New Journal of Physics* **15**, 013047 (2013).
- [42] H. Singh, T. Chakraborty, D. Das, H. S. Jeevan, Y. Tokiwa, P. Gegenwart, and C. Mitra, Experimental quantification of entanglement through heat capacity, *New Journal of Physics* **15**, 113001 (2013).
- [43] S. Aldoshin, E. Fel'dman, and M. Yurishchev, Quantum entanglement and quantum discord in magnetoactive materials, *Low Temperature Physics* **40**, 3 (2014).
- [44] T. Chakraborty, H. Singh, and C. Mitra, Signature of quantum entanglement in $(\text{NH}_4)\text{CuPO}_4 \cdot \text{H}_2\text{O}$, *Journal of Applied Physics* **115** (2014).
- [45] T. Chakraborty, H. Singh, and C. Mitra, Experimental evidences of singlet to triplet transition in a spin cluster compound, *Journal of Magnetism and Magnetic Materials* **396**, 247 (2015).
- [46] H. Singh, T. Chakraborty, P. K. Panigrahi, and C. Mitra, Experimental estimation of discord in an antiferromagnetic Heisenberg compound $\text{Cu}(\text{NO}_3)_2 \cdot 2.5\text{H}_2\text{O}$, *Quantum Information Processing* **14**, 951 (2015).
- [47] S. Sahlng, G. Remenyi, C. Paulsen, P. Monceau, V. Saligrama, C. Marin, A. Revcolevschi, L. Regnault, S. Raymond, and J. Lorenzo, Experimental realization of long-distance entanglement between spins in antiferromagnetic quantum spin chains, *Nature Physics* **11**, 255 (2015).
- [48] P. Hauke, M. Heyl, L. Tagliacozzo, and P. Zoller, Measuring multipartite entanglement through dynamic susceptibilities, *Nature Physics* **12**, 778 (2016).
- [49] E. Garlatti, T. Guidi, S. Ansbro, P. Santini, G. Amoretti, J. Ollivier, H. Mutka, G. Timco, I. Vitorica-Yrezabal, G. Whitehead, *et al.*, Portraying entanglement between molecular qubits with four-dimensional inelastic neutron scattering, *Nature communications* **8**, 14543 (2017).
- [50] E. Garlatti, A. Chiesa, T. Guidi, G. Amoretti, P. Santini, and S. Carretta, Unravelling the spin dynamics of molecular nanomagnets with four-dimensional inelastic neutron scattering, *European Journal of Inorganic Chemistry* **2019**, 1106 (2019).

- [51] W. Y. Kon, T. Krisnanda, P. Sengupta, and T. Paterek, Nonclassicality of spin structures in condensed matter: An analysis of $\text{Sr}_{14}\text{Cu}_{24}\text{O}_{41}$, *Phys. Rev. B* **100**, 235103 (2019).
- [52] G. Mathew, S. L. L. Silva, A. Jain, A. Mohan, D. T. Adroja, V. G. Sakai, C. V. Tomy, A. Banerjee, R. Goreti, A. V. N., R. Singh, and D. Jaiswal-Nagar, Experimental realization of multipartite entanglement via quantum fisher information in a uniform antiferromagnetic quantum spin chain, *Phys. Rev. Res.* **2**, 043329 (2020).
- [53] A. Scheie, P. Laurell, A. M. Samarakoon, B. Lake, S. E. Nagler, G. E. Granroth, S. Okamoto, G. Alvarez, and D. A. Tennant, Witnessing entanglement in quantum magnets using neutron scattering, *Phys. Rev. B* **103**, 224434 (2021).
- [54] F. L. Pratt, F. Lang, W. Steinhardt, S. Haravifard, and S. J. Blundell, Spin dynamics, entanglement, and the nature of the spin liquid state in YbZnGaO_4 , *Phys. Rev. B* **106**, L060401 (2022).
- [55] P. Laurell, A. Scheie, C. J. Mukherjee, M. M. Koza, M. Enderle, Z. Tylczynski, S. Okamoto, R. Coldea, D. A. Tennant, and G. Alvarez, Quantifying and Controlling Entanglement in the Quantum Magnet Cs_2CoCl_4 , *Phys. Rev. Lett.* **127**, 037201 (2021).
- [56] S. Athira, S. L. Silva, P. Nag, S. Lakshmi, S. Kumar, D. P. Panda, S. Das, S. Rajput, A. P. Alex, A. Sundaresan, *et al.*, Bipartite entanglement via distance between the states in a one dimensional spin 1/2 dimer copper acetate monohydrate, *New Journal of Physics* **25**, 103002 (2023).
- [57] A. O. Scheie, E. A. Ghioldi, J. Xing, J. A. Paddison, N. E. Sherman, M. Dupont, L. D. Sanjeewa, S. Lee, A. J. Woods, D. Abernathy, D. M. Pajerowski, T. J. Williams, S. S. Zhang, L. O. Manuel, A. E. Trumper, C. D. Pemmaraju, A. S. Sefat, D. S. Parker, T. P. Devereaux, R. Movshovich, J. E. Moore, C. D. Batista, and D. A. Tennant, Proximate spin liquid and fractionalization in the triangular antiferromagnet KYbSe_2 , *Nature Physics* 10.1038/s41567-023-02259-1 (2023).
- [58] A. Scheie, P. Laurell, E. Dagotto, D. A. Tennant, and T. Roscilde, Reconstructing the spatial structure of quantum correlations (2023), arXiv:2306.11723 [cond-mat.str-el].
- [59] P. Laurell, A. Scheie, E. Dagotto, and D. A. Tennant, Witnessing entanglement and quantum correlations in condensed matter: A review (2024), arXiv:2405.10899 [quant-ph].
- [60] F. D. M. Haldane, 'Luttinger liquid theory' of one-dimensional quantum fluids. I. Properties of the Luttinger model and their extension to the general 1D interacting spinless Fermi gas, *Journal of Physics C: Solid State Physics* **14**, 2585 (1981).
- [61] S.-k. Ma, C. Dasgupta, and C.-k. Hu, Random antiferromagnetic chain, *Phys. Rev. Lett.* **43**, 1434 (1979).
- [62] C. Dasgupta and S.-k. Ma, Low-temperature properties of the random heisenberg antiferromagnetic chain, *Phys. Rev. B* **22**, 1305 (1980).
- [63] D. S. Fisher, Random antiferromagnetic quantum spin chains, *Phys. Rev. B* **50**, 3799 (1994).
- [64] N. Laflorencie, Quantum entanglement in condensed matter systems, *Physics Reports* **646**, 1 (2016).
- [65] K. Uematsu, T. Hikihara, and H. Kawamura, Frustration-induced Quantum Spin Liquid Behavior in the $s = 1/2$ Random-bond Heisenberg Antiferromagnet on the Zigzag Chain, *Journal of the Physical Society of Japan* **90**, 124703 (2021).
- [66] S. Hill and W. K. Wootters, Entanglement of a Pair of Quantum Bits, *Phys. Rev. Lett.* **78**, 5022 (1997).
- [67] W. K. Wootters, Entanglement of formation of an arbitrary state of two qubits, *Phys. Rev. Lett.* **80**, 2245 (1998).
- [68] V. Coffman, J. Kundu, and W. K. Wootters, Distributed entanglement, *Phys. Rev. A* **61**, 052306 (2000).
- [69] M. Imada and M. Takahashi, Quantum transfer monte carlo method for finite temperature properties and quantum molecular dynamics method for dynamical correlation functions, *Journal of the Physical Society of Japan* **55**, 3354 (1986).
- [70] A. Hams and H. De Raedt, Fast algorithm for finding the eigenvalue distribution of very large matrices, *Phys. Rev. E* **62**, 4365 (2000).
- [71] S. Sugiura and A. Shimizu, Thermal pure quantum states at finite temperature, *Phys. Rev. Lett.* **108**, 240401 (2012).
- [72] S. Sugiura and A. Shimizu, Canonical thermal pure quantum state, *Phys. Rev. Lett.* **111**, 010401 (2013).
- [73] H.-K. Lo, T. Spiller, and S. Popescu, *Introduction to quantum computation and information* (World Scientific, 1998).
- [74] L. Gurvits, Classical deterministic complexity of edmonds' problem and quantum entanglement, in *Proceedings of the Thirty-Fifth Annual ACM Symposium on Theory of Computing*, STOC '03 (New York, USA, 2003) pp. 10–19.
- [75] L. Pezzè and A. Smerzi, Quantum theory of phase estimation, in *Atom Interferometry* (IOS Press, 2014) pp. 691–741.
- [76] U. Glaser, H. Büttner, and H. Fehske, Entanglement and correlation in anisotropic quantum spin systems, *Phys. Rev. A* **68**, 032318 (2003).
- [77] L. Amico, A. Osterloh, F. Plastina, R. Fazio, and G. Massimo Palma, Dynamics of entanglement in one-dimensional spin systems, *Physical Review A - Atomic, Molecular, and Optical Physics* **69**, 24 (2004), arXiv:0307048 [quant-ph].
- [78] T. Roscilde, P. Verrucchi, A. Fubini, S. Haas, and V. Tognetti, Studying quantum spin systems through entanglement estimators, *Phys. Rev. Lett.* **93**, 167203 (2004).
- [79] T. J. Osborne and F. Verstraete, General monogamy inequality for bipartite qubit entanglement, *Phys. Rev. Lett.* **96**, 220503 (2006).
- [80] S. Lovesey, *Theory of Neutron Scattering from Condensed Matter: Nuclear scattering*, International series of monographs on physics (Clarendon Press, 1984).
- [81] V. Menon, N. E. Sherman, M. Dupont, A. O. Scheie, D. A. Tennant, and J. E. Moore, Multipartite entanglement in the one-dimensional spin-1/2 Heisenberg antiferromagnet, *Physical Review B* **107**, 54422 (2023).
- [82] T. Giamarchi, *Quantum Physics in One Dimension* (Oxford University Press, 2003).
- [83] I. Affleck, Exact correlation amplitude for the Heisenberg antiferromagnetic chain, *Journal of Physics A: Mathematical and General* **31**, 4573 (1998).
- [84] S. Lukyanov, Low energy effective Hamiltonian for the XXZ spin chain, *Nuclear Physics B* **522**, 533 (1998).

- [85] Y.-R. Shu, D.-X. Yao, C.-W. Ke, Y.-C. Lin, and A. W. Sandvik, Properties of the random-singlet phase: From the disordered heisenberg chain to an amorphous valence-bond solid, *Phys. Rev. B* **94**, 174442 (2016).
- [86] S. J. Gu, H. Q. Lin, and Y. Q. Li, Entanglement, quantum phase transition, and scaling in the XXZ chain, *Physical Review A - Atomic, Molecular, and Optical Physics* **68**, 4 (2003).
- [87] B.-Q. Jin and V. E. Korepin, Localizable entanglement in antiferromagnetic spin chains, *Phys. Rev. A* **69**, 062314 (2004).
- [88] L. Hulthén, *Über das austauschproblem eines kristalles*, Ph.D. thesis, Almqvist & Wiksell (1938).
- [89] I. Affleck, Universal term in the free energy at a critical point and the conformal anomaly, *Phys. Rev. Lett.* **56**, 746 (1986).
- [90] J. A. Hoyos, A. P. Vieira, N. Laflorencie, and E. Miranda, Correlation amplitude and entanglement entropy in random spin chains, *Phys. Rev. B* **76**, 174425 (2007).
- [91] A. Klümper, The spin-1/2 Heisenberg chain: thermodynamics, quantum criticality and spin-Peierls exponents, *THE EUROPEAN PHYSICAL JOURNAL B c EDP Sciences* **5**, 677 (1998).
- [92] G. Refael and J. E. Moore, Entanglement entropy of random quantum critical points in one dimension, *Phys. Rev. Lett.* **93**, 260602 (2004).
- [93] O. A. Starykh, R. R. P. Singh, and A. W. Sandvik, Quantum Critical Scaling and Temperature-Dependent Logarithmic Corrections in the Spin-Half Heisenberg Chain, *Phys. Rev. Lett.* **78**, 539 (1997).
- [94] N. Laflorencie, H. Rieger, A. W. Sandvik, and P. Henelius, Crossover effects in the random-exchange spin- $\frac{1}{2}$ antiferromagnetic chain, *Phys. Rev. B* **70**, 054430 (2004).
- [95] N. Laflorencie, Scaling of entanglement entropy in the random singlet phase, *Physical Review B—Condensed Matter and Materials Physics* **72**, 140408 (2005).
- [96] P. A. Volkov, C.-J. Won, D. I. Gorbunov, J. Kim, M. Ye, H.-S. Kim, J. H. Pixley, S.-W. Cheong, and G. Blumberg, Random singlet state in Ba₅CuIr₃O₁₂ single crystals, *Phys. Rev. B* **101**, 020406 (2020).
- [97] Y.-R. Shu, M. Dupont, D.-X. Yao, S. Capponi, and A. W. Sandvik, Dynamical properties of the $S = \frac{1}{2}$ random Heisenberg chain, *Phys. Rev. B* **97**, 104424 (2018).
- [98] T. Shimokawa, S. Sabharwal, and N. Shannon, in preparation, .
- [99] A. Laeuchli and C. Lhuillier, Dynamical correlations of the kagome $S = 1/2$ heisenberg quantum antiferromagnet, arXiv preprint arXiv:0901.1065 (2009).
- [100] J. Knolle, D. L. Kovrizhin, J. T. Chalker, and R. Moessner, Dynamics of a Two-Dimensional Quantum Spin Liquid: Signatures of Emergent Majorana Fermions and Fluxes, *Phys. Rev. Lett.* **112**, 207203 (2014).
- [101] T. Shimokawa and H. Kawamura, Finite-temperature crossover phenomenon in the $S = 1/2$ antiferromagnetic Heisenberg model on the kagome lattice, *Journal of the Physical Society of Japan* **85**, 113702 (2016).
- [102] M. Kawamura, K. Yoshimi, T. Misawa, Y. Yamaji, S. Todo, and N. Kawashima, Quantum lattice model solver HΦ, *Computer Physics Communications* **217**, 180 (2017).